J. Biochem. **123**, 115-119 (1998)

A Two-Dimensional ^{1}H Detected ^{13}C NMR Investigation of Pyruvate Metabolism in *Halobacterium salinarium*

Ananya Majumdar and Haripalsingh M. Sonawat[1]

Chemical Physics Group, Tata Institute of Fundamental Research, Homi Bhabha Road, Bombay-400 005, India

Received for publication, August 4, 1997

Two-dimensional ^{1}H detected ^{13}C NMR spectroscopy has been used to study the intracellular metabolism of [3-^{13}C]pyruvate in *Halobacterium salinarium*. The method, resulting in considerable improvement in spectral resolution and signal-to-noise ratio, is well suited for studying transient metabolic intermediates. Pyruvate utilization by the bacterium is a double exponential function with rate constants of 49.13 and 4.67×10^{-3} per min. The relative ^{13}C enrichment is the fastest for C-3 glutamate. Glutamate C-4 labeling decreases initially and increases later on during incubation, while glutamine C-3 is high to begin with and exhibits a declining trend. The glutamate labeling indicates a high initial flux through pyruvate carboxylase and extensive randomizing of the label in the tricarboxylic acid cycle.

Key words: ^{13}C NMR, *Halobacterium salinarium*, pyruvate metabolism, tca cycle.

Halobacterium salinarium is an extremely halophilic chemoorganotroph that needs a high concentration of salt for growth and maintenance of cell structure (*1*). Despite the "anoxic" natural habitat that results from high salt concentration, the organism has been described as an obligate aerobe. The enzymes of the tricarboxylic acid (TCA) and glyoxylate cycle are induced only in the presence of acetate in the growth medium (*2-4*). It is, however, of interest to study the TCA and the anaplerotic pathways *in vivo* and to investigate the relative fluxes through pyruvate:ferredoxin oxidoreductase and pyruvate carboxylase. In an earlier study using [2-^{13}C]pyruvate as a substrate we observed the labeling of glutamate in addition to that of lactate and alanine (*5*). Pyruvate:ferredoxin oxidoreductase and pyruvate carboxylase are the major routes for entry of pyruvate into the TCA cycle (Fig. 1). Here we report our observations on the metabolism of [3-^{13}C]-pyruvate in *H. salinarium*. The NMR experiments, performed in intact cells, allowed us (a) to study the metabolism in the cells in an unperturbed manner, and (b) to follow the flow of label from the substrate into intermediates and or products in several metabolic pathways simultaneously. Although this leads to considerable overall broadening of the NMR signals, due to high intracellular concentration of Mn^{2+} (*6*), the method obviates the need for working under conditions optimum for stability of the enzymes involved in the pathways.

[1] To whom correspondence should be addressed. Tel: +91-22-215-2971 (Ext 2271), Fax: +91-22-215-2110/2181, E-mail: hms@tifrvax.tifr.res.in

Abbreviations: FID, free induction decay; HMQC, heteronuclear multiple quantum coherence; NMR, nuclear magnetic resonance; γ, gyromagnetic ratio; S/N, signal-to-noise ratio; TPPI, time proportional phase incrementation; TSP, sodium 3-trimethylsilylpropionate; TCA, tricarboxylic acid cycle.

The conventional methodology for studying metabolic pathways using ^{13}C NMR is through one-dimensional ^{13}C spectra recorded as a function of time. Peaks are assigned to ^{13}C atoms of various substrates and metabolites and the time development of their intensities is used for investigating the relevant metabolic pathways. This method suffers from two basic problems: (a) an inherently poor S/N ratio in ^{13}C spectra and (b) overlap of resonances in one-dimensional spectra. The poor sensitivity necessitates signal averaging for as long as 30 min. The long acquisition periods smear out information regarding transient and/or short-lived metabolites. Essentially, the directly observed ^{13}C spectra possess a very coarse time-resolution. The second problem, of resonance overlap, is typical of one-dimensional spectroscopy and often obscures metabolites with near-degenerate chemical shifts.

In this paper, we present an alternative method for following metabolic pathways, using two-dimensional ^{1}H detected ^{1}H-^{13}C correlated spectroscopy. Since the detected nucleus is ^{1}H, the method is highly sensitive. The inherent signal-to-noise is about 8 times $[(\gamma_H/\gamma_C)^{3/2}]$ more than that of directly observed ^{13}C spectra (*7*). In addition, T_1s of protons are much shorter than those of ^{13}C. Therefore, the relaxation delays between transients are also greatly reduced. In combination, these factors greatly reduce the time needed for acquiring a single one-dimensional ^{1}H detected spectrum (typically, a few seconds) with high sensitivity. The full benefits of this approach are derived through a two-dimensional experiment, *e.g.* HMQC (*8*), which correlates the ^{1}H and ^{13}C shifts in the 2D spectrum. This greatly enhances resolution by separating the ^{13}C shifts in the two-dimensional plane according to the shifts of their attached protons. Since individual FIDs require only a few seconds to be acquired, a complete two-dimensional experiment with sufficient resolution may be performed within 6 to 7 min. This effectively increases the time resolution of the experiments by nearly a factor of

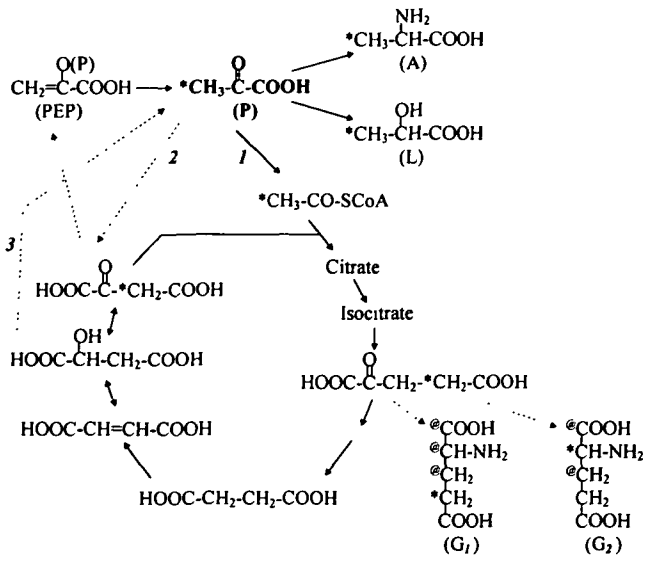

Fig. 1. **Pyruvate metabolism in *H. salinarium*.** 1, pyruvate: ferredoxin oxidoreductase; 2, pyruvate carboxylase; 3, malic enzyme. *Initial and @ subsequent labeling of glutamate carbons through *1* (G_1) and *2* (G_2). The asterisk shown in α-ketoglutarate indicates the label introduced *via* 1, and that in oxaloacetate is from 2. A, alanine; G, glutamate; L, lactate; P, pyruvate; PEP, phosphoenolpyruvate. Dashed arrows indicate anaplerotic reactions.

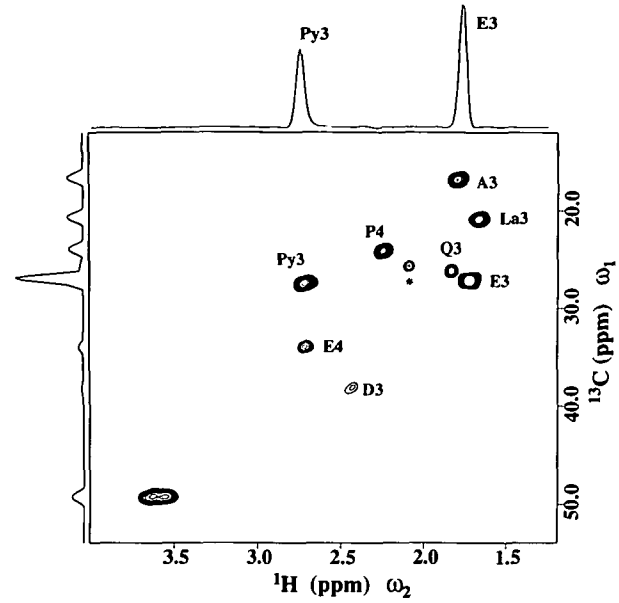

Fig. 2. **^{1}H-^{13}C HMQC spectrum of *H. salinarium* cells.** The cells were incubated with [3-^{13}C]pyruvate for 6 h. The resonance assignments are A3, carbon-3 of alanine; D3, C-3 of aspartate; E3 and E4, C3 and C4 of glutamate, respectively; P4, C4 of proline; Py3, C3 of pyruvate. *Unassigned resonance. A "skyline" projection of the ^{13}C (ω_1) axis and a cross section along the ^{1}H (ω_2) axis are also shown, indicating the high signal-to-noise ratio in the spectrum.

four. Recently, similar applications involving ^{1}H-^{15}N HMQC experiments have been reported for the study of *in vivo* glutamine synthetase activity in rat brain (*9, 10*).

MATERIALS AND METHODS

Chemicals—[3-^{13}C]Pyruvate was procured from Isotec, Miamisburg, OH, USA, and bacteriological peptone was from Oxoid, Hampshire, England. All other chemicals were of analytical grade and were used as supplied.

Cell Culture—*H. salinarium* (earlier *H. halobium*) culture was kindly provided by Prof. A.K. Singh, Department of Chemistry, Indian Institute of Technology, Bombay. It was maintained and propagated in a medium containing 250 g NaCl, 2 g KCl, 20 g $MgSO_4 \cdot 7H_2O$, 10 g glucose and 10 g peptone per liter (*11*). Cells were grown in Erlenmeyer flasks (50 ml culture in 150 ml flask) in a rotary shaker at 37°C and 150 rpm. After incubation for 70 h the culture was diluted 20 times with fresh medium for further propagation. At the end of the incubation period, cells were harvested by centrifugation at $1,200 \times g$ for 30 min and resuspended (25% w/v) in basal salt medium (growth medium without peptone and glucose) prepared in D_2O.

NMR Experiments—NMR experiments were carried out on a Bruker AMX 500 spectrometer, equipped with a broadband inverse-detection probe. The experiments were started by adding solid [3-^{13}C]pyruvate to a 0.5 ml suspension of *H. salinarium* cells in a 5 mm diameter NMR tube. The pulse sequence used was the standard ^{1}H-^{13}C HMQC sequence (*8*). For each spectrum, 512 (t_2, complex) $\times$ 108 (t_1, real) data points were acquired, with the minimum phase cycle of two transients per t_1 increment. Quadrature detection along ω_1 was achieved using the TPPI method (*12*). Spectral widths along ω_2 and ω_1 were (7,042 Hz, 14 ppm) and (7,546 Hz, 60 ppm), respectively. Presaturation of the H_2O signal was achieved with a 20 Hz rf field applied for 1 s. The relaxation delay (including the acquisition and presaturation periods) between transients was 2 s. Low-power ^{13}C decoupling (2.5 kHz) was used during acquisition. This had to be carefully optimized since sample heating due to high salt concentrations may lead to degradation of spectral quality during the course of the experiment. The total acquisition time for each spectrum was about 7 min. Spectra were processed using Felix 2.30 software (Biosym). Peaks were assigned either by comparison with those reported in the literature or by recording spectra of authentic metabolites in basal salt medium. Chemical shifts are reported with respect to TSP.

RESULTS

Two-Dimensional Spectra—Figure 2 shows a contour plot of the HMQC spectrum of *H. salinarium* cells, grown in complex medium supplemented with glucose, after incubation with [3-^{13}C]pyruvate for 6 h. Resonances corresponding to C-3 of alanine (A3) and lactate (La3) are observed in addition to those of C-3 (E3) and C-4 (E4) of glutamate, C-3 of glutamine (Q3), C-4 of proline (P4), and unutilized C-3 pyruvate (Py3). Minor signals are also observed for C-3 of aspartate (D3). The high resolution of the spectrum is clearly evident. As the projection along the ^{13}C (ω_1) axis shows, the peaks due to C-3 of glutamate and C-3 of pyruvate could not have been resolved in the corresponding ^{13}C one-dimensional spectrum alone. On the top of the plot, a cross section along ω_2 is shown, indicating the high S/N ratio of the spectrum.

Figure 3, a-d, shows stacked plots of the annotated region of the spectrum in Fig. 2, recorded at intervals of (a) 13, (b)

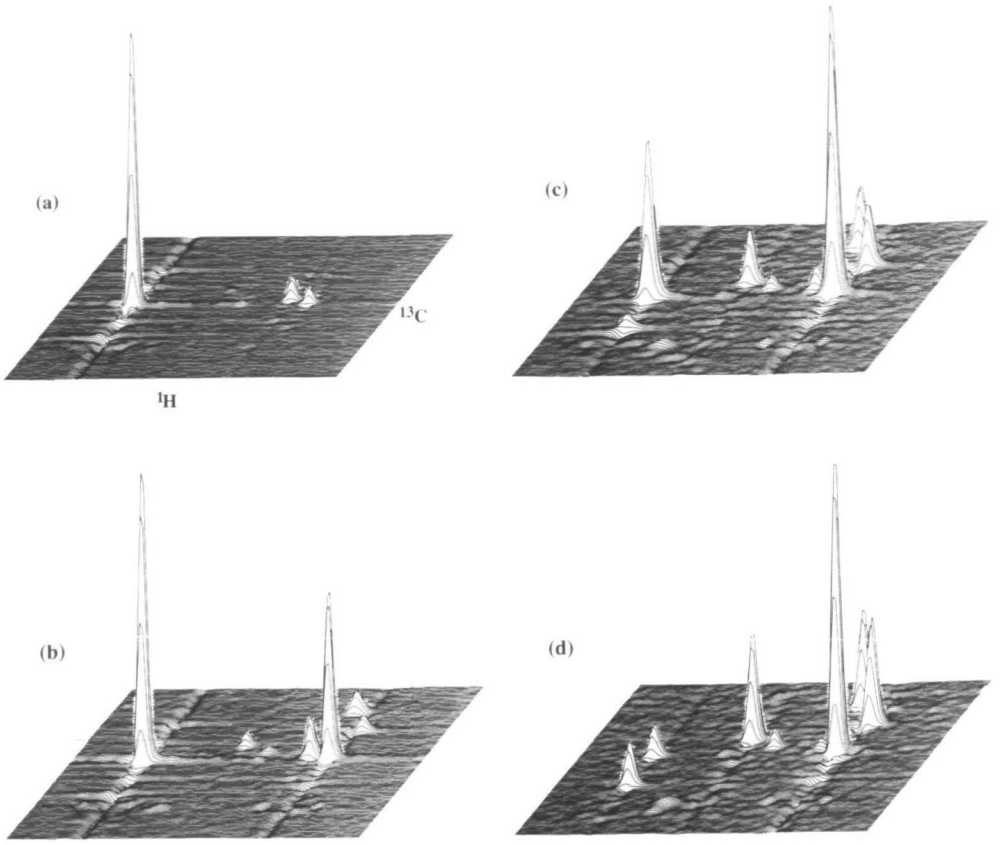

Fig. 3. **Stacked plots of pyruvate metabolism in *H. salinarium*.** The cells were incubated with [3-^{13}C]pyruvate as mentioned in Fig. 2a and 2D HMQC spectra were acquired at various time intervals. The plots represent the annotated region (1.45-3.0 ppm ω_2, 15-40 ppm ω_1) at (a) 13, (b) 74, (c) 257, and (d) 726 min after the addition of labeled pyruvate to the cell suspension. The indicated time is the time at the end of the acquisition of a 2D spectrum.

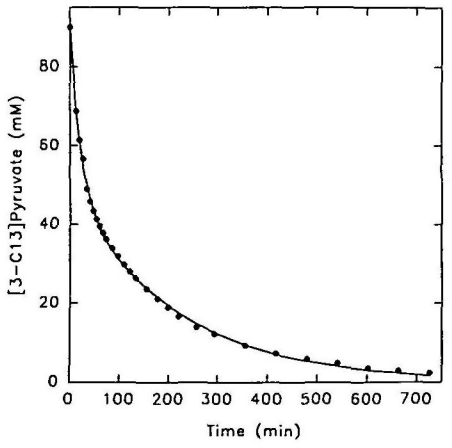

Fig. 4. **Utilization of [3-^{13}C]pyruvate by *H. salinarium*.** The initial concentration of the added substrate was equated to the volume of its 2D NMR signal determined as mentioned in "MATERIALS AND METHODS." All subsequent concentrations were calculated by normalizing the peak volumes to the initial concentration. Circles are data points and the solid line is a double exponential fitting.

74, (c) 257, and (d) 726 min after addition of labeled pyruvate. In Fig. 3a, the dominant signal is due to the substrate, but it is evident that within the first 10-15 min, metabolites are already beginning to appear in small quantities. The appearance and subsidence of peaks corresponding to various metabolites may be seen in Fig. 3, b-d.

Pyruvate Uptake—The utilization of [3-^{13}C]pyruvate by *H. salinarium* is shown in Fig. 4. No difference was observed in the chemical shifts of the pyruvate in the extracellular medium and that inside the cells. Figure 4 therefore represents the change in total concentration of the labeled pyruvate with time regardless of transport across the cell membrane. As mentioned earlier, solid [3-^{13}C]pyruvate was added to a 0.5 ml cell suspension. The initial phase corresponds to a faster utilization as compared to the later slower uptake of the substrate. The data were fitted to a two-exponential decay function and the rates were 49.13 and 4.67×10^{-3} per min.

Production of Metabolites—Time dependences of the ^{13}C enrichments of various positions in the metabolites were monitored by following the appearance of resonances of these metabolites. The results are shown in Fig. 5. The concentrations of lactate labeled at C-3, generated by lactate dehydrogenase reaction, and alanine C-3, a product of either amination of pyruvate and/or a transamination reaction, increased in parallel during the later phase of the experiment. The initial rise of labeled alanine was, however, faster than that of lactate. The rise time and maximum concentration were the same in both cases. The concentration of glutamate labeled at C-3 rose sharply in the initial stages, reached a maximum after about 3 h, and decreased gradually thereafter. In contrast, glutamate C-4 concentration decreased initially, reached a minimum and then showed an increasing trend throughout the experiment. Proline C-4 concentration increased gradually during the experiment. The initial concentration of glutamine C-3 was high and showed a declining trend in the experiment.

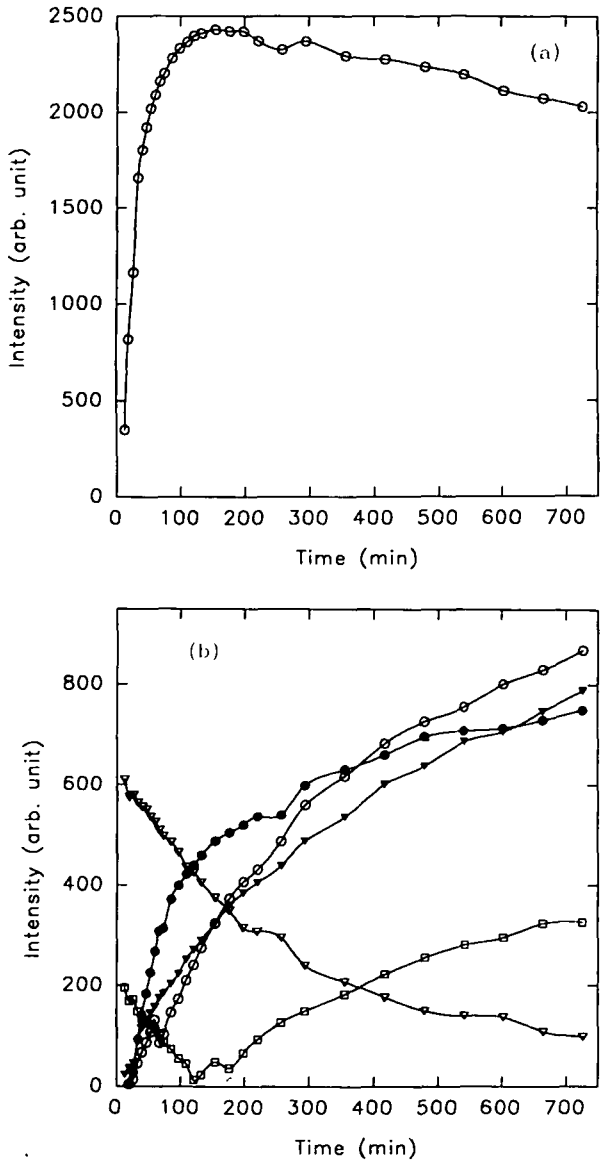

Fig. 5. **Time evolution of the ^{13}C enrichment of metabolites in *H. salinarium* incubated with [3-^{13}C]pyruvate.** Volumes of the 2D NMR resonances have been directly plotted against time. a: C-3 glutamate; b: ○, C-3 lactate; ▼, C-3 alanine; ●, C-4 proline; □, C-4 glutamate; and ▽, C-3 glutamine.

DISCUSSION

Pyruvate, added to a cell suspension of *H. salinarium*, is utilized in several different metabolic pathways (Fig. 1). The condition of the cell suspension seemed to be partly aerobic. The limited oxygen tension results in the production of lactate. Labeled alanine, observed in the NMR spectra, is a result of single-step transaminase and or amination reactions. The intensity of the lactate signal reflects the extent to which oxygen is limited in the experiments. In other experiments where the oxygen tension was further reduced, the lactate concentration was found to be high. The concentration of alanine was, however, not affected in these studies.

Pyruvate enters the Kreb's (TCA) cycle through two routes. One of them is the pyruvate dehydrogenase reaction which generates acetyl-CoA, followed by its condensation with oxaloacetate to form citrate. The condensation reaction is catalyzed by citrate synthase. The pyruvate dehydrogenase reaction is well documented and known to exist in many prokaryotes and most eukaryotes. In *H. salinarium*, as in other halophilic bacteria, the conversion of pyruvate to acetyl-CoA is catalyzed by pyruvate:ferredoxin oxidoreductase (*13, 14*). This enzyme utilizes ferredoxin as the coenzyme for transfer of electrons instead of NAD^+ and FAD. The other route is pyruvate carboxylase, which is utilized by most heterotrophs and eukaryotes for carbon dioxide assimilation (*15-19*); its presence in halobacteria has been reported (*20*). Our observations on labeling of glutamate suggest that both these routes are available for the entry of pyruvate into the TCA cycle in *H. salinarium*. The time profiles of the metabolites (Fig. 5, a and b) have some unusual features. First, the enrichment at C-3 glutamate is the fastest when compared to the other carbons of glutamate. Second, the labelings of C-4 of glutamate and proline are parallel, except in the initial phase. These observations suggest that the relative flux of pyruvate carboxylase is high during the initial phase and that most of the label enters the TCA cycle through this route. Also, a major fraction of [3-^{13}C]pyruvate label entering *via* pyruvate:ferredoxin oxidoreductase is recycled. These two factors result in rapid build up of C-3 glutamate. With continued incubation, the flux through pyruvate carboxylase and the extent of recycling decrease while the flux of pyruvate:ferredoxin oxidoreductase increases. This is reflected by the increasing concentration of C-4 glutamate in the latter phase of incubation. We had shown earlier that, at the steady state, 10% of the total label enters the TCA cycle through pyruvate carboxylase, with 90% of the label going through pyruvate:ferredoxin oxidoreductase (data not shown). Furthermore, the extent of recycling (the fraction of labeled oxaloacetate condensing with acetylCoA to form citrate) of the label is 40%. In addition, a progressively incremental amount of C-4 glutamate is sequestered for C-4 proline generation. This again is evident from the almost parallel evolution of the concentrations of the two labeled metabolites (Fig. 5a).

[2-^{13}C]Acetyl-CoA, formed from [3-^{13}C]pyruvate, leads to C-4 glutamate during the first third of the TCA cycle (Fig. 1a). C-3 glutamate is generated by, (i) recycling and scrambling of this label during subsequent cycles and, (ii) entry of the label (from pyruvate) through the pyruvate carboxylase reaction and its complete randomization due to substantial back-reaction through the (fumarase/succinate dehydrogenase) fumarate/succinate stage before it proceeds to condensation with acetyl-CoA (Fig. 1b). Glutamate C-3 is thus the combined result of the α-ketoglutarate produced by extensive cycling of the label in the TCA cycle and the high flux through pyruvate carboxylase in the initial stage of incubation (Fig. 5a).

A high initial glutamine C-3 concentration is indicative of a high glutamine synthetase activity during this period. The enzyme has been reported to be under negative allosteric modulation by alanine (*15*). In our experiments we observed an increase in the level of alanine with time (Figs. 3 and 5). Although there are no independent reports of alanine-mediated allosteric inhibition of glutamine syn-

thetase in *H. salinarium*, our observations seem to be consistent with this phenomenon.

At present, we are investigating the multiple labeling in glutamate, specifically as affected by growth conditions of this halophilic archaebacterium. The TCA cycle enzymes in the bacterium exist in the cytosol except for succinate dehydrogenase, which has been reported both in cytosol and membrane fraction (*21*). Although we do not expect any kind of organization of the cycle enzymes as has been reported in other organisms and higher eukaryotic systems (*22-24*), this has yet to be investigated. The strikingly different pattern of evolution of C-3 labeled glutamate and glutamine and C-4 glutamate suggests changing relative fluxes of pyruvate carboxylase and pyruvate:ferredoxin oxidoreductase, and randomizing of the label in the TCA cycle.

Finally, for the first time, the efficacy of using two-dimensional ^{1}H detected ^{13}C NMR spectroscopy to trace the time-course of intracellular substrate metabolism in intact cells has been demonstrated in this study. High signal-to-noise ratio is achievable in a relatively short experimental time (6 to 7 min), thus improving the accuracy of quantification and the time resolution of the kinetics, with concomitant gains in spectral resolution. The limitation of this method is the inability to obtain information regarding $^{13}C=O$ carbons since they do not possess attached protons. Appropriate pulse techniques are being developed to address this problem.

We are grateful to the National Facility for High Field NMR located at T.I.F.R., Bombay for machine time on the 500 MHz NMR spectrometer and we thank the facility staff for their cooperation.

REFERENCES

1. Hochstein, L.I. (1988) The physiology and metabolism of the extremely halophilic bacteria in *Halophilic Bacteria* (Rodriguez-Valera, F., ed.) Vol. 2, pp. 67-83, CRC Press, Boca Raton
2. Aitken, D.M. and Brown, A.D. (1969) Citrate and glyoxylate cycles in the halophile *Halobacterium salinarium*. *Biochim. Biophys. Acta* **177**, 351-354
3. Danson, M.J. (1988) Archaebacteria: The comparative enzymology of their central metabolic pathways. *Adv. Microbial. Physiol.* **29**, 165-231
4. Danson, M.J., Black, S.C., Woodland, D.L., and Wood, P.A. (1985) Citric acid cycle enzymes of the archaebacteria: citrate synthase and succinate thiokinase. *FEBS Lett.* **179**, 120-124
5. Bhaumik, S.R. and Sonawat, H.M. (1994) Pyruvate metabolism in *Halobacterium salinarium* studied by intracellular ^{13}C NMR spectroscopy. *J. Bacteriol.* **176**, 2172-2176
6. Quirk, P.G. and Campbell, I.D. (1990) ^{31}P and ^{39}K nuclear magnetic resonance spectroscopy studies of halobacterial bioenergetics. *Biochim. Biophys. Acta* **1019**, 81-90
7. Kessler, H., Gehrke, M., and Griesinger, C. (1988) Two-dimensional NMR spectroscopy: Background and overview of the experiments. *Angew. Chem. Int. Ed. Engl.* **27**, 490-536
8. Bax, A., Griffey, R.H., and Hawkins, B.L. (1983) Correlation of proton and nitrogen-15 chemical shifts by multiple quantum NMR. *J. Magn. Reson.* **55**, 301-315
9. Kanamori, K., Ross, B.D., and Kuo, E.L. (1995) Dependence of *in vivo* glutamine synthetase activity on ammonia concentration in rat brain studied by ^{1}H-^{15}N heteronuclear multiple-quantum coherence-transfer NMR. *Biochem. J.* **311**, 681-688
10. Kanamori, K., Ross, B.D., and Tropp, J. (1995) Selective *in vivo* observation of [5-^{15}N]glutamine amide protons in rat brain by ^{1}H-^{15}N heteronuclear multiple-quantum-coherence transfer NMR. *J. Magn. Reson. Ser B* **107**, 107-115
11. Oesterhelt, D. and Stoeckenius, W. (1974) Isolation of the cell membrane of *Halobacterium halobium* and its fractionation into red and purple membrane. *Methods Enzymol.* **31**, 667-678
12. Marion, D. and Wüthrich, K. (1983) Application of phase sensitive two-dimensional correlated spectroscopy (COSY) for measurements of ^{1}H-^{1}H spin-spin coupling constants in proteins. *Biochem. Biophys. Res. Commun.* **113**, 967-974
13. Kerscher, L. and Oesterhelt, D. (1977) Ferredoxin is the coenzyme of α-ketoacid oxidoreductases in *Halobacterium halobium*. *FEBS Lett.* **83**, 197-201
14. Kerscher, L. and Oesterhelt, D. (1981) Purification and properties of two 2-oxoacid:ferredoxin oxidoreductases from *Halobacterium halobium*. *Eur. J. Biochem.* **116**, 595-600
15. Brand, A., Engelmann, J., and Leibfritz, D. (1992) A ^{13}C NMR study on fluxes into the TCA cycle of neuronal and glial cell lines and primary cells. *Biochemie* **74**, 941-948
16. Hartman, R.E. (1970) Carbon dioxide fixation by extracts of *Streptococcus faecalis* var. *liquefaciens*. *J. Bacteriol.* **102**, 341-346
17. Jans, A.W.H. and Leibfritz, D. (1989) A ^{13}C NMR study on fluxes into the Krebs cycle of rabbit renal proximal tubular cells. *NMR Biomed.* **1**, 171-176
18. Jans, A.W.H. and Willem, R. (1989) A ^{13}C NMR investigation of the metabolism of amino acids in renal proximal convoluted tubules of normal and streptozotocin-treated rats. *Biochem. J.* **263**, 231-241
19. Lachica, R.V.F. and Hartman, P.A. (1968) Carbon dioxide fixation and the synthesis of aspartic acid by *Streptococcus faecium* var. *durans*. *Biochem. Biophys. Res. Commun.* **32**, 691-695
20. Rawal, N., Kelkar, S.M., and Altekar, W. (1988) Alternative routes of carbohydrate metabolism in halophilic archaebacteria. *Ind. J. Biochem. Biophys.* **25**, 674-686
21. Gradin, C.H., Hederstedt, L., and Baltscheffsky, H. (1985) Soluble succinate dehydrogenase from halophilic archaebacterium, *Halobacterium halobium*. *Arch. Biochem. Biophys.* **239**, 200-205
22. Evans, C.T., Sumegi, B., Srere, P.A., Sherry, A.D., and Malloy, C.R. (1993) [^{13}C]Propionate oxidation in wild type and citrate synthase mutant *Escherichia coli:* evidence for multiple pathways of propionate utilization. *Biochem. J.* **291**, 927-932
23. Sumegi, B., Sherry, A.D., and Malloy, C.R. (1990) Channeling of TCA cycle intermediates in cultured *Saccharomyces cerevisiae*. *Biochemistry* **29**, 9106-9110
24. Tompa, P., Batke, J., Ovadi, J., Welch, G.R., and Srere, P.A. (1987) Quantitation of the interaction between citrate synthase and malate dehydrogenase. *J. Biol. Chem.* **262**, 6089-6092